Segmentation of the Full Myocardium in Echocardiography Using Constrained Level-Sets

Martino Alessandrini[1], Thomas Dietenbeck[2], Daniel Barbosa[2,3], Jan D'hooge[3], Olivier Basset[2], Nicolò Speciale[1], Denis Friboulet[2], Olivier Bernard[2]

[1]ARCES-DEIS, University of Bologna, Bologna, Italy
[2]CREATIS LRMN, University of Lyon, Villeurbanne, France
[3]Department of Cardiovascular Diseases, Catholic University of Leuven, Leuven, Belgium

Abstract

In echocardiography, left ventricle detection is a common practice in order to retrieve indexes of myocardial health. Although a great attention has been given to the segmentation of the endocardium, very limited literature addresses the detection of both endo- and epicardial contours. Hereto, in this study we propose an original level-set technique specifically designed for the detection of the whole myocardium in short-axis ultrasound scans. A localized version of standard region-based methods is adopted, and allows to deal with low-contrast boundaries. Moreover, shape prior information is efficiently embedded in the evolution equation, thereby preventing the detection of undesired structures, like papillary muscles. An evaluation is presented on a set of 40 frames from 5 different patients. The proposed method is shown to be a reliable tool for an accurate segmentation of the full myocardium on ultrasound scans.

1. Introduction

Left ventricle segmentation is fundamental in order to retrieve important indexes of heart function, such as ejection fraction and cardiac output. These measures are often obtained via manual segmentation, which is subjective and time consuming, due to the intrinsic low SNR of ultrasound scans. To reduce inter- and intra-observer variability in border detection and to speed up the segmentation process, an automated procedure is desirable [1].

While great attention has been given to the segmentation of the endocardium, very limited literature addresses the detection of the epicardium [1–3]. This is due to the fact that signal dropouts and complex interactions between the ultrasonic pulse and the tissue make the epicardial contour appear highly heterogeneous and discontinuous. Nevertheless, a trustful detection of both structures has a high clinical relevance, since it would allow the computation of fundamental parameters as the ventricular mass, which has been proven to be an important precursor for a variety of conditions such as cardiomyopathy, hypertension and valvular disease. In this context, we have recently proposed in [4] a level-set approach for simultaneous segmentation of endo- and epicardium from parasternal short-axis (SAx) views. Although good performances was observed, the algorithm suffered from undesired irregularities in the final solution, due to the attachment of the active contour to undesired structures, like papillary muscles. In this work we propose a method to avoid this effect by embedding a priori knowledge on the myocardial shape in the segmentation process. Specifically, we assume that the myocardial shape may be approximated by two ellipses, an inner and an outer one (in the sequel, we will refer to the shape comprised between two ellipses as annular). This assumption is indeed well supported by observation on SAx views [5].

In order to address the shape prior segmentation of both contours with a single level set function we introduce in this paper an original parametric formulation of the distance from an annular shape as well as a fast solution to the least-squares fitting of such patterns. A validation is presented which shows that the resulting algorithm is a reliable tool to segment the full myocardium. In particular, a comparison with the results obtained with [4] shows the important improvement due to the shape prior information.

The remainder of the paper is structured as follows. In section 2 the level-set equation for the presented framework is derived, with a focus on how the shape prior is handled. In section 3, several implementation issues are addressed. In section 4 the validation is presented.

2. Proposed method

2.1. Level-set framework

Let $\Omega \subset \mathbb{R}^2$ denote the image space. In the level-set formalism, the evolving interface $\Gamma \subset \mathbb{R}^2$ is represented

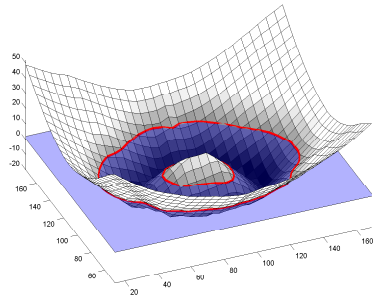

Figure 1. Example of level set function used in this work. The zero level is represented as a red bold line and provides the 2 contours corresponding to the boundary of the annular target.

as the zero level-set of a Lipschitz-continuous function $\phi : \Omega \rightarrow \mathbb{R}$. The problem of segmenting one object from the background is then handled by the evolution of one level-set driven by the minimization of a specific energy criterion; its steady state partitions the image into two regions that delimit the boundaries of the object to be segmented. Since we are addressing the joint detection of two separate contours, i.e. endo- and epicardium, we adopt a ϕ function with a disjoint zero-level, as the one in Fig. 1.

Regarding the energy criterion, as in [6], we adopt the following general expression:

$$E = E_{\text{data}} + \alpha \cdot E_{\text{shape}} \tag{1}$$

where E_{data} represents the data attachment term, driving the segmentation to particular image features, and E_{shape} is a shape prior term, preserving the similarity between the moving interface and the reference model.

2.2. Data attachment term

The data attachment term we adopt in this work is directly derived from the energy criterion presented in [4]. For matter of space, in this section we only present the basic equations. The interested reader is referred to [4] for a more detailed explanation.

In [4] we adopted a localized version of standard region-based approaches [7] in order to deal with the heterogeneous properties of the epicardial contour. The Bhattacharyya coefficient $\mathcal{B}(p_1, p_2)$ was adopted to drive the segmentation process, which is a measure of the superposition between two probability density functions (pdfs) p_1 and p_2. Then the resulting algorithm proceeded by seeking the maximal statistical separation between target, i.e. the myocardium, and background. The energy criterion we adopted writes as:

$$E_{\text{data}} = \int_{\Omega} \delta(\phi(\mathbf{x})) \int_{\Omega} W(\mathbf{x}, \mathbf{y}) \mathcal{B}(p_{\text{in}}, p_{\text{out}}) d\mathbf{y} d\mathbf{x} \tag{2}$$

where $W(\cdot)$ is a binary mask defining, for every point $\mathbf{x}$ on the active contour, the region on which the curve velocity is computed and p_{in} and p_{out}, are the pdfs describing the gray scale pixel distribution inside and outside the moving interface.

As proposed in [8], we assume a Fisher-Tippet probability density function to model the pdf of the log-compressed echo signal, i.e.:

$$p(I|\sigma) = 2 \exp\left([2I - \ln(2\sigma^2)] - \exp\left([2I - \ln(2\sigma^2)]\right)\right), \tag{3}$$

where I is the pixel intensity and σ is the parameter of the distribution. Substituting (3) in (2) we derived the following level-set equation:

$$\frac{\partial \phi}{\partial \tau}(\mathbf{x}) = f(\mathbf{x}) \cdot \delta(\phi(\mathbf{x})) \tag{4}$$

where $\delta(\cdot)$ is the Dirac delta function and

$$f(\mathbf{x}) = \int_{\Omega} \left(W(\mathbf{x}, \mathbf{y})\, \delta(\phi(\mathbf{y})) \frac{(\sigma_{\mathbf{x},\text{o}} \sigma_{\mathbf{x},\text{i}})(\sigma_{\mathbf{x},\text{o}}^2 - \sigma_{\mathbf{x},\text{i}}^2)}{(\sigma_{\mathbf{x},\text{i}}^2 + \sigma_{\mathbf{x},\text{o}}^2)^2} \cdot \right. \tag{5}$$

$$\left. \cdot \left\{ \frac{1}{|\Omega_{\mathbf{x},\text{o}}|} \left[\frac{e^{2I(\mathbf{x})} - 1}{2\sigma_{\mathbf{x},\text{o}}} - 1 \right] + \frac{1}{|\Omega_{\mathbf{x},\text{i}}|} \left[\frac{e^{2I(\mathbf{x})} - 1}{2\sigma_{\mathbf{x},\text{i}}} - 1 \right] \right\} \right) d\mathbf{y}$$

The sets $\Omega_{\mathbf{x},\text{i}}$ ($\Omega_{\mathbf{x},\text{o}}$) contains the pixels belonging to the intersection between the localizing mask and the inside (outside) of the moving interface and $\sigma_{\mathbf{x},\text{i}}$ and $\sigma_{\mathbf{x},\text{o}}$ correspond to the ML estimates of the distribution parameters on $\Omega_{\mathbf{x},\text{i}}$ and $\Omega_{\mathbf{x},\text{o}}$ respectively.

2.3. Shape prior term

In this work we adopt the following shape-prior term:

$$E_{\text{shape}} = \int_{\Omega} \Psi^2(\mathbf{x}, \boldsymbol{\lambda}) ||\nabla \phi(\mathbf{x})|| \delta(\phi(\mathbf{x})) \tag{6}$$

where $\Psi(\mathbf{x}, \boldsymbol{\lambda})$ is the implicit function representing the distance of a point $\mathbf{x}$ to the annular shape defined by the parameters $\boldsymbol{\lambda}$. Clearly (6) reads as a measure of the distance between the active contour and the prior shape, and therefore imposes a similarity between the segmentation result and the prior itself. We propose here to adopt the following parametric expression for Ψ:

$$\Psi(\mathbf{x}, \boldsymbol{\lambda}) = \max\{\mathcal{E}(\mathbf{x}, \boldsymbol{\lambda}_{\text{out}}), -\mathcal{E}(\mathbf{x}, \boldsymbol{\lambda}_{\text{in}})\} \tag{7}$$

where $\boldsymbol{\lambda}_{\text{in}}$ and $\boldsymbol{\lambda}_{\text{out}}$ represent the parameters of the inner and outer ellipses, and $\mathcal{E}$ is the algebraic distance of a point to the ellipse, represented by the standard quadratic equation for conic sections.

The minimization of (6) is addressed in a two phase scheme. Specifically, keeping $\boldsymbol{\lambda}$ fixed, ϕ is evolved according to the level-set equation:

$$\frac{\partial \phi}{\partial \tau} = \delta(\phi(\mathbf{x})) g(\mathbf{x}, \boldsymbol{\lambda}) \tag{8}$$

where

$$g(\mathbf{x},\boldsymbol{\lambda}) = \left\{ 2\Psi \frac{\nabla\Psi\cdot\nabla\phi}{||\nabla\phi||} + \Psi^2 \mathrm{div}\left(\frac{\nabla\phi}{||\nabla\phi||}\right)\right\} \quad (9)$$

where the dependence of ϕ and Ψ on $\mathbf{x}$ has been omitted for compactness of notation. Then, keeping ϕ fixed, $\boldsymbol{\lambda}$ is updated according to the following least-squares fitting problem:

$$\boldsymbol{\lambda} = \underset{\boldsymbol{\lambda}'}{\mathrm{argmin}} \oint_{\Gamma} \Psi^2(s,\boldsymbol{\lambda}')ds = \underset{\boldsymbol{\lambda}'}{\mathrm{argmin}} \sum_{\mathbf{x}_i\in\Gamma} \Psi^2(\mathbf{x}_i,\boldsymbol{\lambda}') \quad (10)$$

By noting that $||\nabla\phi|| = 1$ because of the signed distance property [9], then (10) corresponds to the exact minimization of (6) w.r.t. $\boldsymbol{\lambda}$. The rightmost of (10) is justified by the fact that the image space is in practice discrete.

In the following subsection we propose a fast solution to the least squares fitting problem in (10), which can be employed for implementing efficiently the parameters update step.

2.3.1. Least-squares fitting of annular shapes.

Considering (7), we can rewrite the sum in (10) as:

$$J(\mathbf{x},\boldsymbol{\lambda}) = \sum_{\mathbf{x}\in\Gamma_{\mathrm{A}}} \mathcal{E}^2(\mathbf{x},\boldsymbol{\lambda}_{\mathrm{out}}) + \sum_{\mathbf{x}\in\Gamma_{\mathrm{B}}} \mathcal{E}^2(\mathbf{x},\boldsymbol{\lambda}_{\mathrm{in}}) \quad (11)$$

where the partition $\Gamma = \{\Gamma_{\mathrm{A}},\Gamma_{\mathrm{B}}\}$ has been introduced

$$\Gamma_{\mathrm{A}}(\boldsymbol{\lambda}_{\mathrm{in}},\boldsymbol{\lambda}_{\mathrm{out}}) = \{\mathbf{x}\in\Gamma | \mathcal{E}(\mathbf{x},\boldsymbol{\lambda}_{\mathrm{out}}) \geq -\mathcal{E}(\mathbf{x},\boldsymbol{\lambda}_{\mathrm{in}})\} \quad (12)$$
$$\Gamma_{\mathrm{B}}(\boldsymbol{\lambda}_{\mathrm{in}},\boldsymbol{\lambda}_{\mathrm{out}}) = \{\mathbf{x}\in\Gamma | \mathcal{E}(\mathbf{x},\boldsymbol{\lambda}_{\mathrm{out}}) < -\mathcal{E}(\mathbf{x},\boldsymbol{\lambda}_{\mathrm{in}})\}$$

From this formulation we observe that (11) can be minimized by fitting two separate ellipses on Γ_{A} and Γ_{B}, for which fast direct solvers exist [10]. We thus propose to minimize J with the algorithm summarized in Table 1, which proceeds by alternatively fitting two separate ellipses on Γ_{A} and Γ_{B} and then updating the two sets according to (12). By doing so, the energy J is ensured to decrease at each step. In Table 1 we call fitLS the function performing the direct least-squares ellipse fitting described in [10].

On all our simulations, the described fitting algorithm is found to converge in less then 5 iterations, which makes the amount of computation due to the solution of (10) essentially negligible.

Table 1. Least Squares Fitting Algorithm

Input data: $\hat{\boldsymbol{\lambda}}_{\mathrm{in}}^{(0)}, \hat{\boldsymbol{\lambda}}_{\mathrm{out}}^{(0)}$, k=1, tol = 1e-2

Initialization:

$E^{(0)} = J\left[\hat{\boldsymbol{\lambda}}_{\mathrm{in}}^{(0)}, \hat{\boldsymbol{\lambda}}_{\mathrm{out}}^{(0)}\right];$

$\Gamma_{\mathrm{A}}^{(0)} = \Gamma_{\mathrm{A}}\left[\hat{\boldsymbol{\lambda}}_{\mathrm{in}}^{(0)}, \hat{\boldsymbol{\lambda}}_{\mathrm{out}}^{(0)}\right]; \quad \Gamma_{\mathrm{B}}^{(0)} = \Gamma_{\mathrm{B}}\left[\hat{\boldsymbol{\lambda}}_{\mathrm{in}}^{(0)}, \hat{\boldsymbol{\lambda}}_{\mathrm{out}}^{(0)}\right];$

while $\epsilon >$ tol **do**:

$\hat{\boldsymbol{\lambda}}_{\mathrm{in}}^{(\mathrm{k})} = \mathrm{fitLS}\left[\Gamma_{\mathrm{B}}^{(\mathrm{k}-1)}\right]; \quad \hat{\boldsymbol{\lambda}}_{\mathrm{out}}^{(\mathrm{k})} = \mathrm{fitLS}\left[\Gamma_{\mathrm{A}}^{(\mathrm{k}-1)}\right];$

$\Gamma_{\mathrm{A}}^{(\mathrm{k})} = \Gamma_{\mathrm{A}}\left[\hat{\boldsymbol{\lambda}}_{\mathrm{in}}^{(\mathrm{k})}, \hat{\boldsymbol{\lambda}}_{\mathrm{out}}^{(\mathrm{k})}\right]; \quad \Gamma_{\mathrm{B}}^{(\mathrm{k})} = \Gamma_{\mathrm{B}}\left[\hat{\boldsymbol{\lambda}}_{\mathrm{in}}^{(\mathrm{k})}, \hat{\boldsymbol{\lambda}}_{\mathrm{out}}^{(\mathrm{k})}\right];$

$E^{(k)} = J\left[\hat{\boldsymbol{\lambda}}_{\mathrm{in}}^{(\mathrm{k})}, \hat{\boldsymbol{\lambda}}_{\mathrm{out}}^{(\mathrm{k})}\right];$

$\epsilon = ||E^{(\mathrm{k})} - E^{(\mathrm{k}-1)}||/||E^{(\mathrm{k}-1)}||; \quad$ k=k+1;

end while

3. Implementation issues

We implemented our level-set evolution equation using a standard finite difference scheme [9], where ϕ is represented by a signed distance function. In order to improve efficiency, we only compute values of ϕ in a narrow band around the zero level set [9]. Consequently, we re-initialize ϕ every iteration using a fast marching scheme.

The final curve velocity is given by $f(\mathbf{x}) + \alpha \cdot g(\mathbf{x},\boldsymbol{\lambda})$, where f and g are defined as in (5) and (9). A value of 0.8 was assigned to α in all the experiments presented in the paper.

Furthermore, let us note that the adoption of a localized framework [7] imposes an initialization not too far from the desired solution, in order to obtain meaningful results. The following simple procedure is thus followed to initialize our algorithm. The user is asked to place six points: five points are used to set an initial ellipse for the epicardial wall and a last point is needed to obtain the internal concentric ellipse representing the endocardium. The union of the two ellipses is taken as initialization. In the result section we display the five points on the epicardium as green dots and the one on the endocardium as a green triangle. Finally, the localizing approach is implemented by assuming as mask W a disk whose radius was experimentally set to 10 pixels.

4. Results

As a preliminary evaluation, the algorithm was validated on a set of B-mode images acquired on 5 different patients. For each sequence 8 frames equally spaced within one cardiac cycle were considered, for a total of 40 scans. Data were acquired using a Toshiba Powervision 6000 (Toshiba Medical Systems Europe, Zoetermeer, the Netherlands) equipped with a 3.75 MHz-probe. The algorithm was initialized by a non-expert user as described in the previous

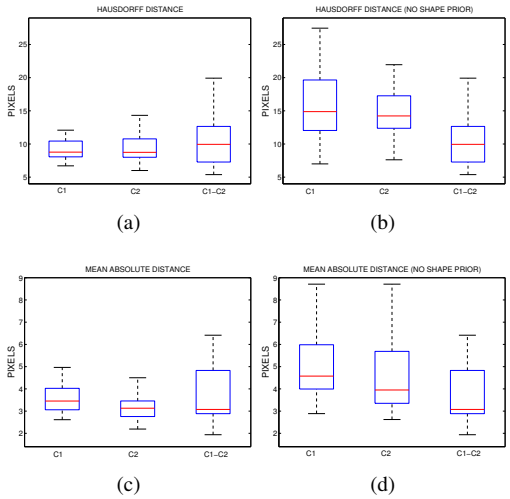

Figure 2. On each box the central mark is the median and the edges are the 25th and 75th percentiles, the whiskers are the 5th and 95th percentiles. In (a) and (c) the results obtained using the shape prior, in (b) and (d) the results when the shape prior is not taken into account. The labels C1 and C2 correspond to the comparison of the segmentation results with the reference provided by the first or the second cardiologist while label C1-C2 corresponds to the comparison between the contours provided by the two cardiologists themselves.

section. Manual segmentation drawn by two expert cardiologists was used as reference.

We assessed the performances of the algorithm by measuring Mean Absolute Deviation (MAD) and Hausdorff Distance (HD) between automatic and reference contours, as well as the correlation coefficient (R) between the areas they enclose. To study the effect of the shape information we run our algorithm both with and without including such term in the evolution equation. A segmentation result example is given in Fig.3.

When the shape information is considered we obtained MAD $= 3.1 \pm 0.5$ pixels and HD $= 9.2 \pm 2$ pixels. The correlation coefficient was R $= 0.98$. When the shape is not considered the performances decrease giving MAD $= 5 \pm 1.4$, HD $= 15.6 \pm 4.8$ and R $= 0.94$. From the comparison of these results with the inter-observer variability measured between the two manual contours, given by MAD = 3.7 ± 1.2 and HD = 10.6 ± 3.7, we can deduce the suitability of the presented shape prior segmentation framework in producing trustful results.

A box plot representation of the complete set of results is shown in Fig.2.

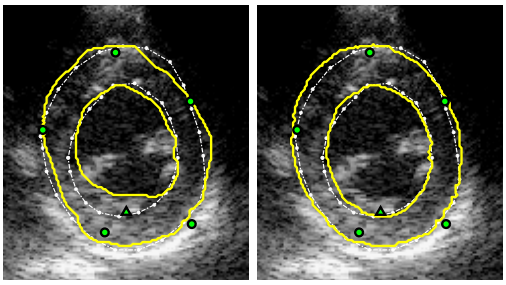

Figure 3. In (a) result without the shape prior, in (b) result with the shape prior. Dashed white contour is the manual reference, the bold yellow one is the detected contour. Green spots are the initialization. We measured HD=13.5 and MD=5.5 for (a), and HD=8.1 and MD=3.3 for (b). All these values are expressed in pixels.

5. Conclusions

We described a level-set approach for segmentation of the full myocardium in echocardiography. The results show that the proposed method in realistic clinical data is feasible and accurate.

References

[1] Noble JA, Boukerroui D. Ultrasound image segmentation: A survey. IEEE TMI 2006;25(8):987–1010.

[2] Dias JMB, Leitao JLM. Wall position and thickness estimation from sequences of echocardiographic images. IEEE TMI 1996;15(1):25–38.

[3] Chalana V, Linker DT, Haynor DR, Kim Y. A multiple active contour model for cardiac boundary detection on echocardiographic sequences. IEEE TMI 1996;15(3):290–298.

[4] Alessandrini M, Friboulet D, Basset O, D'hooge J, Bernard O. Level-set segmentation of myocardium and epicardium in ultrasound images using localized bhattacharyya distance. In Proc. IEEE IUS. 2009; .

[5] Taron M, Paragios N, Jolly M. Border detection on short axis echocardiographic views using a region based ellipse-driven framework. In MICCAI. 2004; 443–450.

[6] Chen Y, Tagare HD, Thiruvenkadam S, Huang F, Wilson D, Gopinath KS, Briggs RW, Geiser EA. Using prior shapes in geometric active contours in a variational framework. IJCV 2002;50:315–328.

[7] Lankton S, Tannenbaum A. Localizing region-based active contours. IEEE TIP 2008;17(11):2029–2039.

[8] Michailovich O, Adam D. Robust estimation of ultrasound pulses using outlier-resistant de-noising. IEEE TMI 2003; 22(3):368–381.

[9] Osher SJ, Fedkiw RP. Level Set Methods and Dynamic Implicit Surfaces. Springer, 2002.

[10] Fitzgibbon AW, Pilu M, Fisher RB. Direct least square fitting of ellipses. IEEE Trans on PAMI 1999;21(5):476–480.